nature portfolio

https://doi.org/10.1038/s41586-021-03275-y

Supplementary information

BNT162b vaccines protect rhesus macaques from SARS-CoV-2

In the format provided by the authors and unedited

Supplementary Figure 1

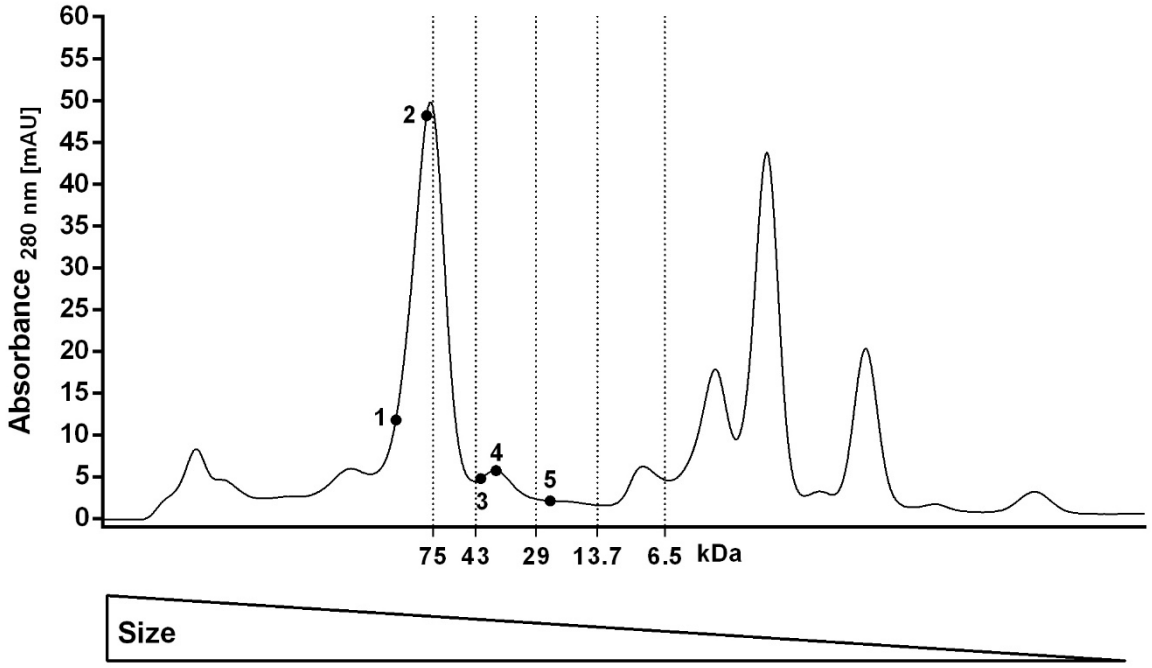

Supplementary Figure 1. Size exclusion chromatography of medium from BNT162b1 RNA-transfected cells.

Concentrated medium of HEK293T cells transfected with BNT162b1 RNA formulated with a transfection reagent (BNT162b1 RNA) was applied to a size exclusion chromatography column, calibrated using protein size standards (75, 43, 29, 13.7 and 6.5 kDa). Numbered dots indicate fractions that were further analysed by western blot.

Supplementary Figure 2

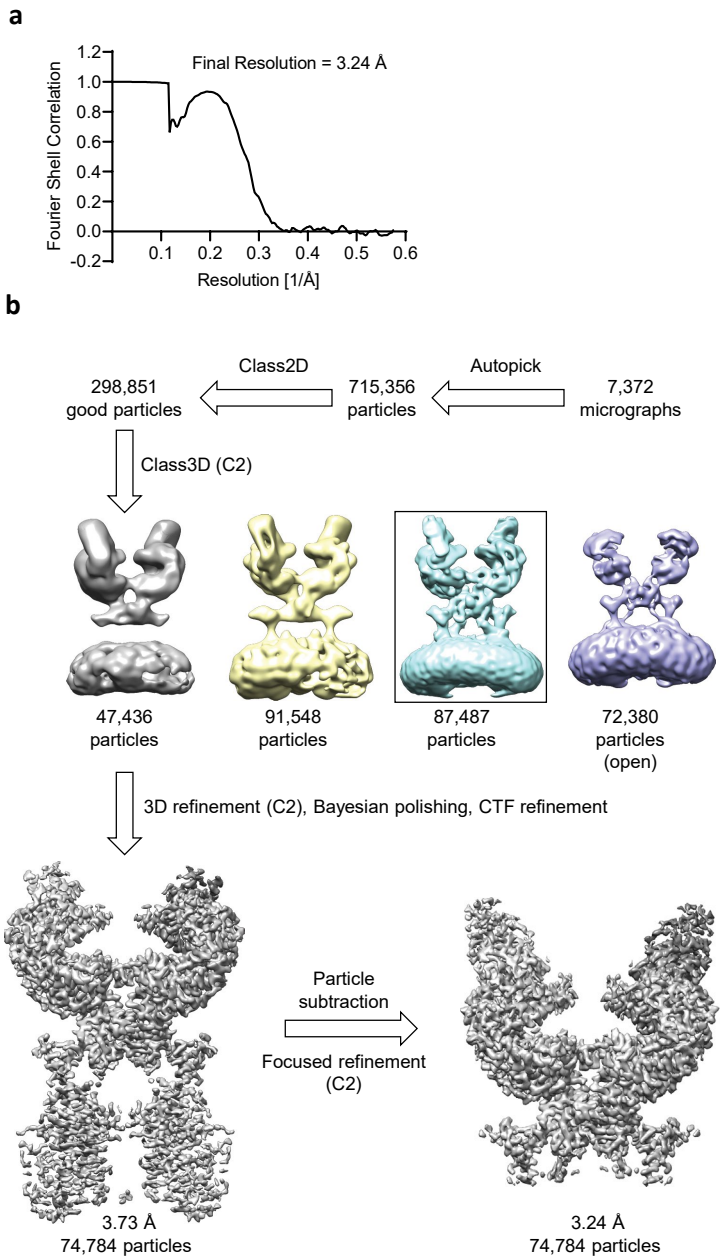

Supplementary Figure 2. Supporting data for cryo-EM of the trimerized RBD in complex with receptor.

a, Fourier shell correlation curve from RELION focused gold-standard refinement of the ACE2/B^{0}AT1/RBD-trimer ternary complex. **b**, Flowchart for cryo-EM data processing of the complex. CTF, contrast transfer function. C2 symmetry applied during classification and refinement.

Supplementary Figure 3

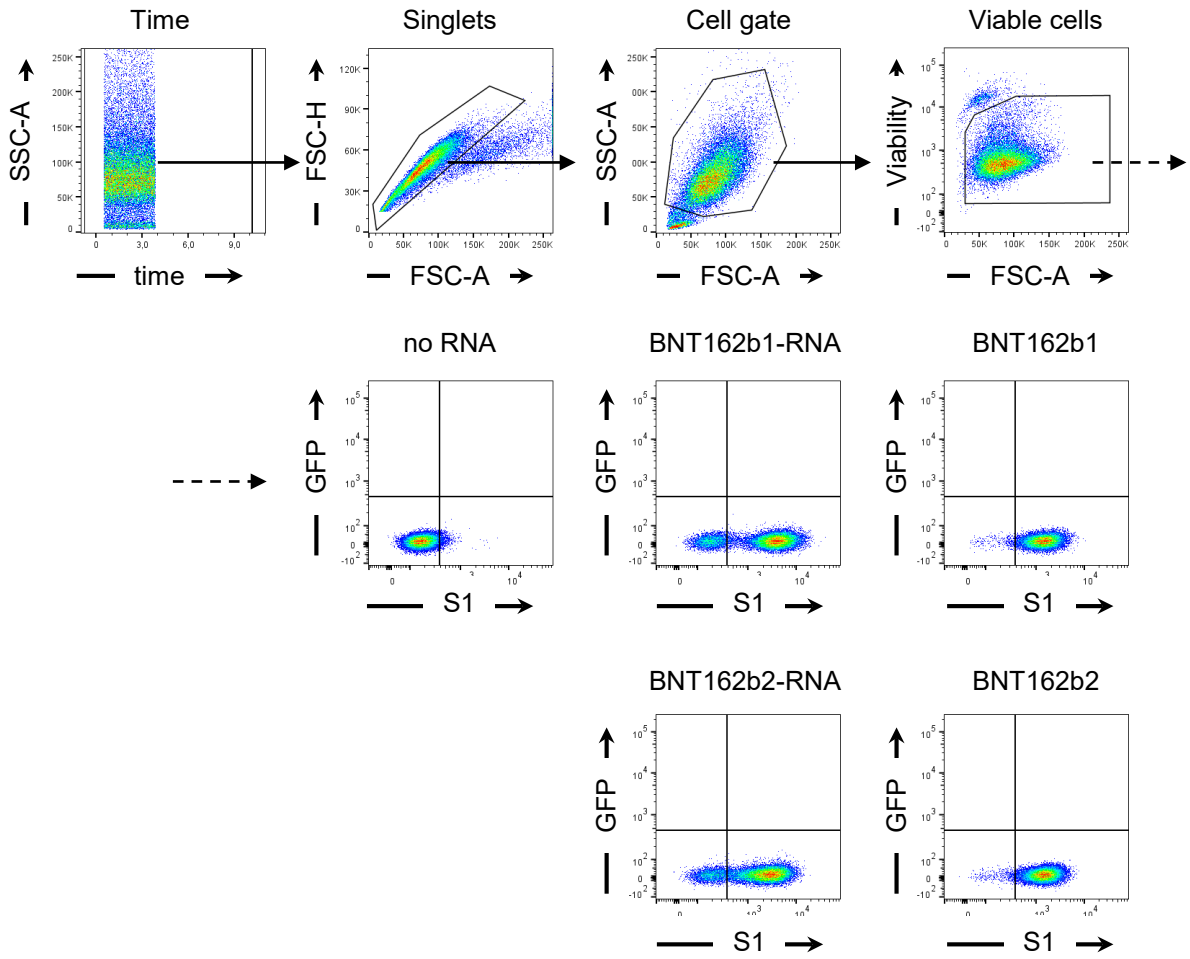

Supplementary Figure 3. Gating strategy for flow cytometry analysis of data shown in Extended Data Figure 1a.

Flow cytometry gating strategy for the identification of HEK293T cells transfected with BNT162b1 or BNT162b2, or BNT162b1-RNA or BNT162b2-RNA using a transfection reagent or no RNA (control). $S1^+$ HEK293T cells were gated within single, viable HEK293T cells.

Supplementary Figure 4

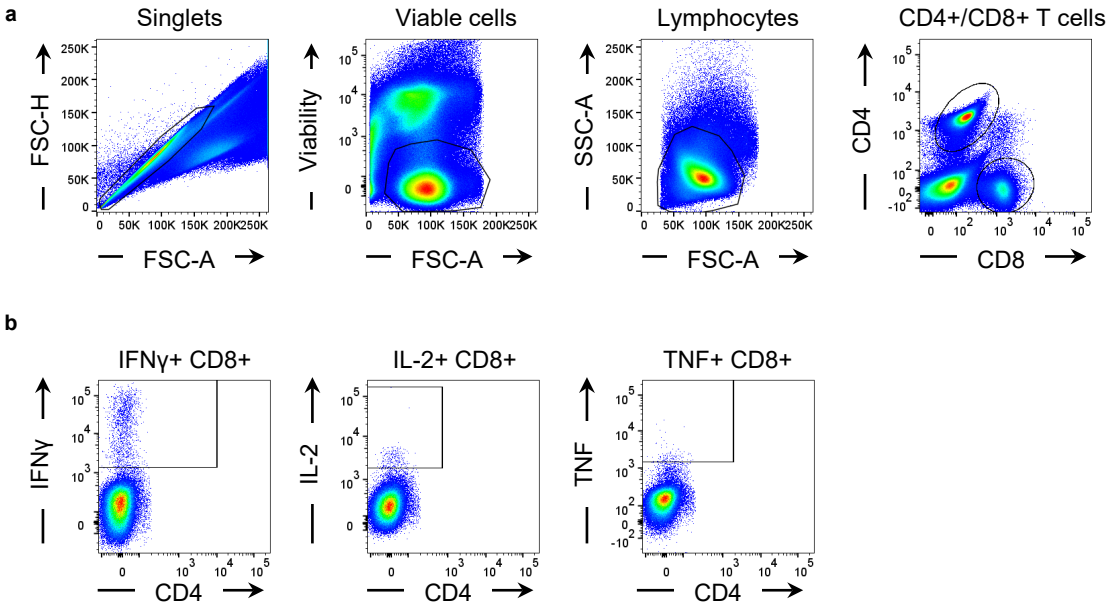

Supplementary Figure 4. Gating strategy for flow cytometry analysis of mouse data shown in Extended Data Figure 4 b.

Flow cytometry gating strategy for the identification of IFNγ, IL-2, and TNF secreting $CD8^+$ T cells in the mouse spleen. **a,** $CD8^+$ T cells were gated within single, viable lymphocytes. **b,** Gating of IFNγ, IL-2 and TNF in $CD8^+$ T cells.

Supplementary Figure 5

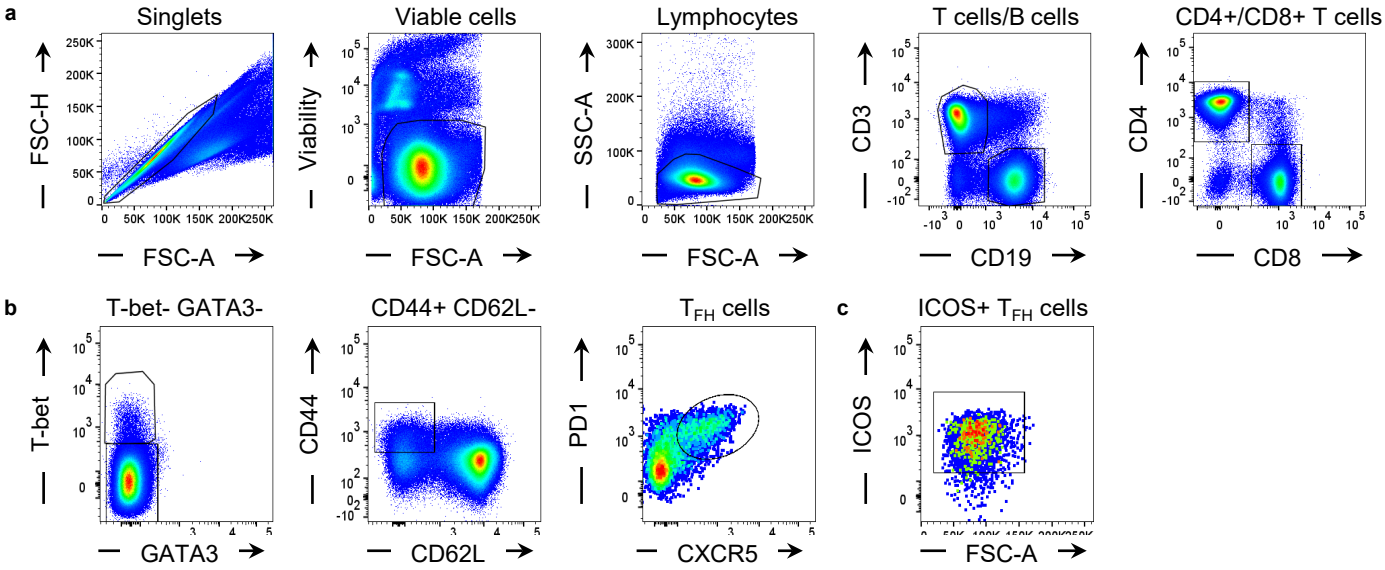

Supplementary Figure 5. Gating strategy for flow cytometry analysis of T-cell phenotypes in murine lymph nodes and spleen shown in Extended Data Figure 4 c and d.

Flow cytometry gating strategy for identification of T_{FH} cells, activated T cells and B cells in lymph nodes and the spleen. **a**, $CD3^{+}CD19^{-}$ T cells were gated within single, viable lymphocytes. $CD4^{+}$ and $CD8^{+}$ T cells were gated from $CD3^{+}$ cells. **b**, T_{FH} cells were gated from $CD4^{+}$ T cells and defined as $CD4^{+}$ T-bet^{-} $GATA3^{-}$ $CD44^{+}$ $CD62L^{-}$ $PD\text{-}1^{+}$ $CXCR5^{+}$ cells.

Supplementary Figure 6

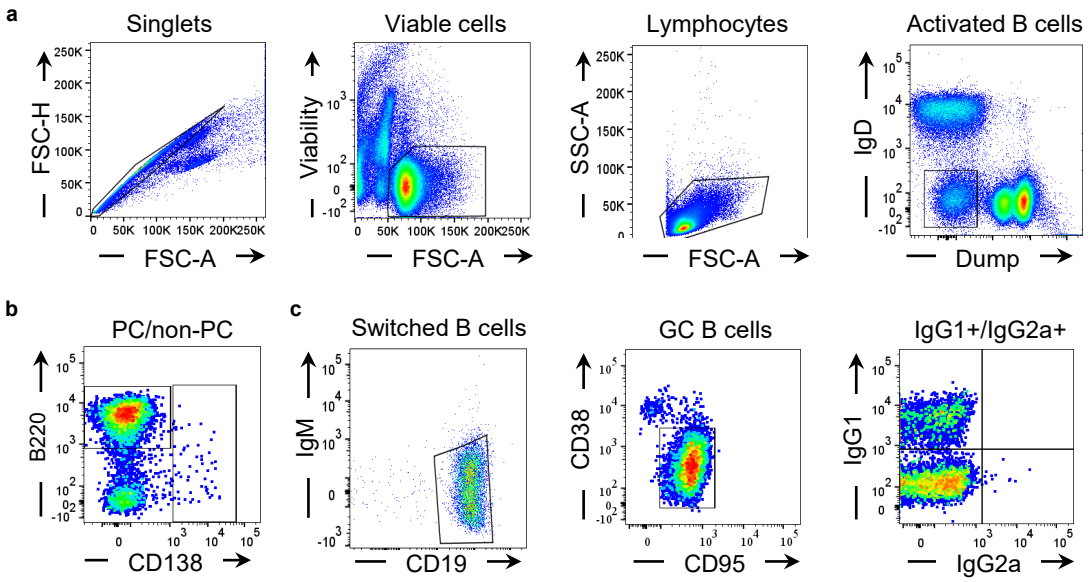

Supplementary Figure 6. Gating strategy for flow cytometry analysis of B-cell subtypes in murine lymph nodes and spleen shown in Extended Data Figure 4 c and d.

Flow cytometry gating strategy for the identification of B cells in lymph nodes and the spleen. **a,** Activated B cells were gated within single, viable lymphocytes and defined as IgD-Dump (CD4, CD8, F4/80, GR-1)$^{-}$ cells. **b,** Plasma cells (PC) were gated from activated B cells and defined as CD138^{+} B220$^{low/-}$ cells. **c,** Switched B cells were gated from non-PC and defined as CD19^{+} CD138^{-} IgM^{-}. Germinal centre (GC) and IgG1^{+} and IgG2a^{+} B cells were gated from switched B cells and defined as CD19^{+} IgM^{-} CD38^{-} CD95^{+} and CD19^{+} IgM^{-} IgG1^{+}/IgG2a^{+}, respectively.

Supplementary Figure 7

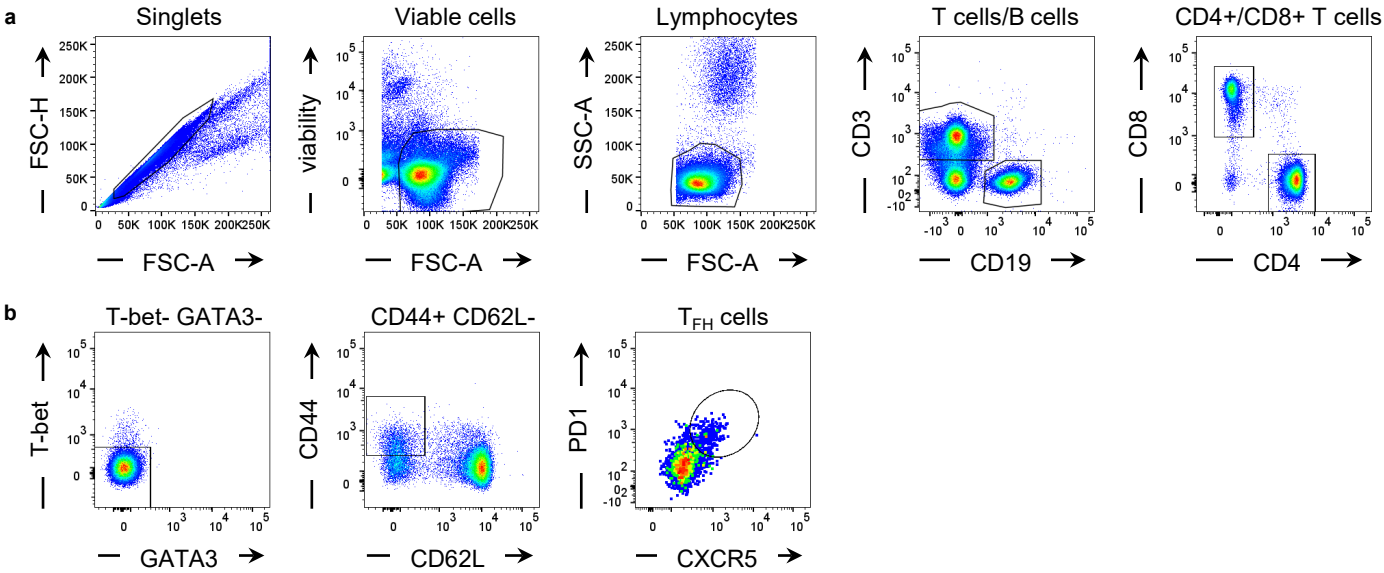

Supplementary Figure 7. Gating strategy for flow cytometry analysis of T-cell phenotypes in mouse peripheral blood shown in Extended Data Figure 4 e.

Flow cytometry gating strategy for the identification of T cells, B cells and T_{FH} cells in peripheral blood. **a,** $CD3^+$ $CD19^-$ T cells were gated within single, viable lymphocytes. $CD4^+$ and $CD8^+$ T cells were gated from $CD3^+$ $CD19^-$ cells. **b,** T_{FH} cells were gated from $CD4^+$ T cells and defined as $CD4^+$ T-bet^- $GATA3^-$ $CD44^+$ $CD62L^-$ $PD\text{-}1^+$ $CXCR5^+$ cells.

Supplementary Figure 8

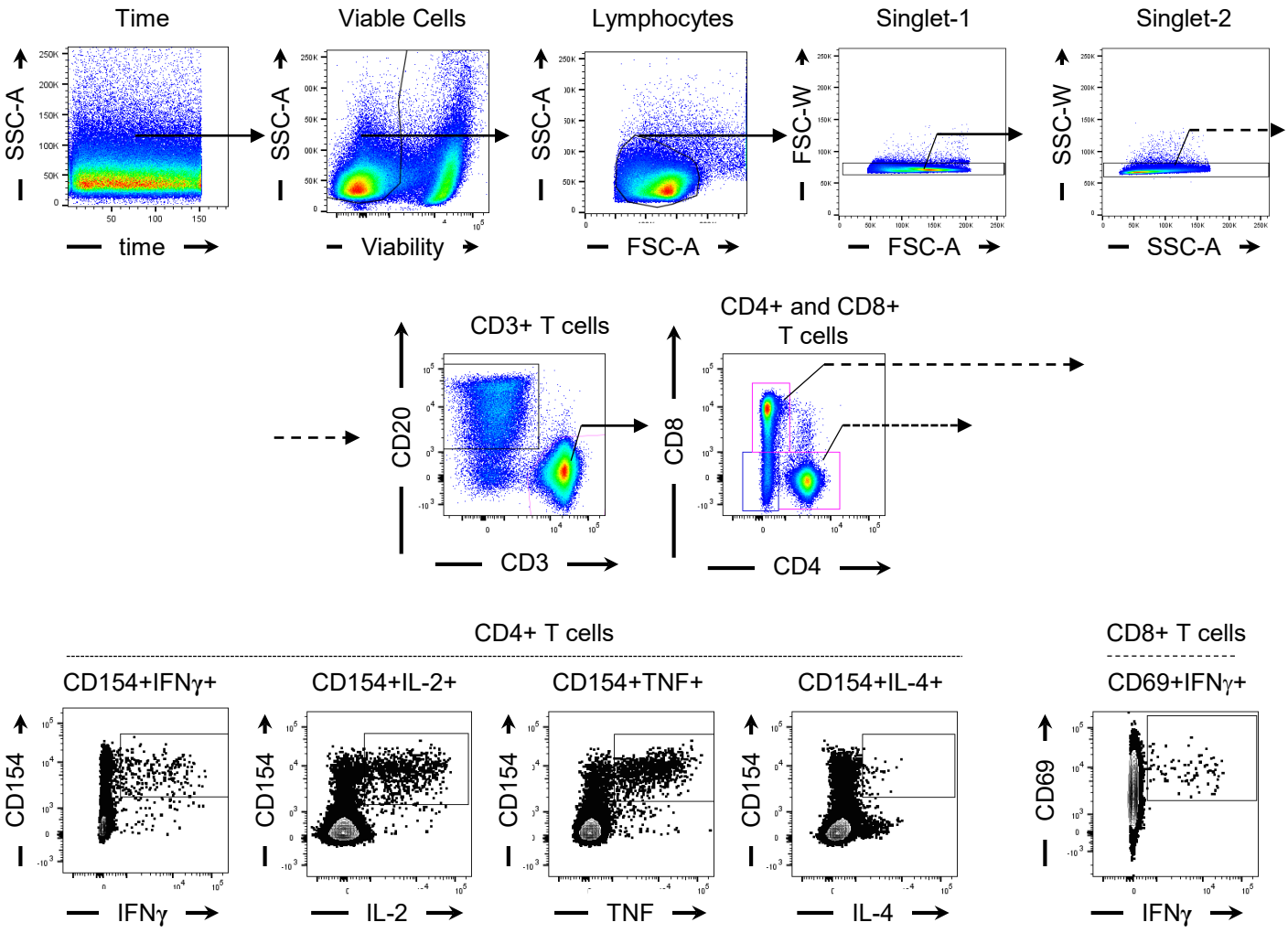

Supplementary Figure 8. Gating strategy for rhesus macaque flow cytometry analysis of data shown in Extended Data Figure 5 b-d.

Flow cytometry gating strategy for identification of spike-specific SARS-CoV-2 modRNA vaccine BNT162b2-induced T cells. Starting with events acquired with a constant flow stream and fluorescence intensity, viable cells, lymphocytes and single events were identified and gated (upper row, left to right). Within singlet lymphocytes, $CD20^-$ $CD3^+$ T cells were identified and gated into $CD4^+$ T cells and CD8+ T cells (middle row). Antigen-specific CD4+ T cells were identified by gating on CD154 and cytokine-positive cells, and CD8+ T cells were identified by gating on CD69 and cytokine-positive cells. The antigen-specific cells were used for further analysis (bottom row).